Biochemistry and Biophysics Reports 1 (2015) 97–107

Contents lists available at ScienceDirect

Biochemistry and Biophysics Reports

journal homepage: www.elsevier.com/locate/bbrep

Molten globule nature of *Plasmodium falciparum* P2 homo-tetramer

Pushpa Mishra [a], Sinjan Choudhary [b], Sujoy Mukherjee [c], Disha Sengupta [d], Shobhona Sharma [d], Ramakrishna V. Hosur [a,b,*]

[a] Department of Chemical Sciences, Tata Institute of Fundamental Research, Mumbai 400005, Maharashtra, India
[b] UM-DAE Centre for Excellence in Basic Sciences, Mumbai University Campus, Mumbai 400098, Maharashtra, India
[c] Structural Biology and Bioinformatics Division, Indian Institute of Chemical Biology, Kolkata 700032, West Bengal, India
[d] Department of Biological Sciences, Tata Institute of Fundamental Research, Mumbai 400005, Maharashtra, India

ARTICLE INFO

Article history:
Received 4 February 2015
Received in revised form
20 March 2015
Accepted 23 March 2015
Available online 31 March 2015

Keywords:
NMR
Plasmodium falciparum P2 (PfP2)
PfP2 structure
Molten globule
Folding and dynamics

ABSTRACT

The P2 protein in *Plasmodium falciparum* has a high tendency to oligomerize, which seems to drive many of its non-ribosomal functions. During nuclear division of the parasite inside RBC, P2 translocates to the RBC surface as a tetramer. From a systematic study using variety of biophysical techniques, NMR spectral characteristics and relaxation dispersion measurements under different conditions of pH and/or urea concentrations, we deduce that (i) PfP2, an almost entirely helical protein, forms a molten globule monomer at low pH, (ii) at physiological pH, and at micro-molar concentrations, PfP2 is a stable tetramer wherein two dimmers associate sideways with close packing of helices at the interface, and (iii) the molten globule characteristic of the monomer is preserved in the tetramer. This dynamism in the structure of PfP2 may have functional implications since it is known that different kinds of oligomers are transiently formed in the parasite.

1. Introduction

Plasmodium falciparum P2 is a ribosomal stalk protein. In higher eukaryotes P1 and P2 proteins interact with P0 forming a pentameric P0-$(P1/P2)_2$ complex and are collectively known as P-proteins [1,2]. Interestingly, *Plasmodium falciparum* P2 (PfP2) is known to be involved in non-ribosomal functions as well and this seems to be associated with its tendency to homo-oligomerize [3]. Malaria parasites develop within the erythrocytes where P2 protein within the parasite body remains largely monomeric until the onset of cell division [3]. P2 protein alone translocates to the infected RBC surface for 6–8 h prior to nuclear division and this translocation is concomitant with extensive oligomerization in the parasite body. The amount of P2 protein is also found to oscillate with the highest amount of P2 protein being formed at 24 h PMI. Within the erythrocytic development cycle of 48 h in synchronized *Plasmodium falciparum* cells, the high concentration of PfP2 protein and its extensive oligomerization mainly at 24 h PMI indicates a definitive role for PfP2 oligomerization, the precise nature of which is yet to be elucidated. At that point a large number of SDS-resistant higher oligomers of P2 protein are detected, but on the infected-erythrocyte surface, only the SDS-resistant homo-tetrameric form of P2 is found [3].

Recent observations have shown that the recombinant human P2 protein is stable as a dimer in solution and this has 69% sequence similarity with PfP2 [4]. In the presence of P1 (25% sequence similarity with P2) of the same species, it forms a stable heterodimer [5]. However, interestingly the core structure in both these homo and hetero-dimers is identical [4,5]. A very recent report on the *Plasmodium* P-protein assembly demonstrated a lack of stable hetero-dimeric complex of P1/P2 proteins, indicating a distinct behavior of these *Plasmodium* proteins [6]. In this study it was observed that PfP1 and PfP2 proteins do not form hetero-dimers, and that in the presence of all three P-proteins, the assembly of pentameric P0-$(P1/P2)_2$ occurred directly, bypassing the stable hetero-dimeric complex.

In this paper we have tried to investigate by NMR and other biophysical methods the structural and dynamic characteristics of PfP2 at residue level detail. This has been challenging since the NMR spectra of PfP2 do not show more than half the number of expected peaks, which is in contrast to the situation in human P2 protein. Nevertheless, we have been able to show that the stable unit of PfP2 in solution in-vitro is a tetramer at micro-molar concentrations. Using a strategy of partially unfolding the tetramer for observing NMR signals from all the residues, gathering insights into structural and motional transitions, and based on the published dimeric structure of human P2 protein, we propose a model for the structure of the PfP2-tetramer.

* Corresponding author at: Department of Chemical sciences, Tata Institute of Fundamental Research, Mumbai 400005, Maharashtra, India.
E-mail address: hosur@tifr.res.in (R.V. Hosur).

http://dx.doi.org/10.1016/j.bbrep.2015.03.010

2. Materials and methods

2.1. Protein expression and purification

Protein expression and purification has been described elsewhere [7,8]. Isotopically enriched (^{15}N or ^{15}N and ^{13}C) PfP2 was prepared using M9 media containing $^{15}NH_4Cl$ and ^{13}C glucose as the sole sources of nitrogen and carbon, respectively. The purified protein was concentrated to ~1 mM concentration. Sample was then exchanged to 6 M, 5 M and 4 M urea solutions prepared in 100 mM MES buffer containing 150 mM NaCl and 1 mM DTT adjusted to pH 5.6. Urea concentration was calculated using refractive index measurements. The NMR samples (containing 10% D_2O (v/v)) were allowed to attain equilibrium before starting the experiments.

2.2. NMR spectroscopy

Relaxation dispersion NMR measurements were performed at 25° C on Bruker 500 MHz and 800 MHz equipped with a room temperature probe and cryoprobe with triple axis gradients. Other relaxation experiments were recorded on Bruker 800 MHz equipped with a cryo probe with triple axis gradients. All pulse schemes were gradients and sensitivity enhanced and employed water flip back for optimal water suppression [9–11]. Milliseconds (ms) conformational dynamics can be quantified using CPMG relaxation dispersion NMR techniques [12–14]. In all these experiments constant time relaxation compensated pulse sequence developed by Kay and coworkers were used [15]. These are essentially Car–Purcell–Meiboom–Gill (CPMG) ^{15}N T_2 measurements recorded by varying the number of π pulses in a constant time (T_{relax}) spin echo sequence. A ^1H continuous spin-lock field is applied during the ^{15}N CPMG π pulse train. A constant duty cycle was maintained by incorporating additional RF pulses following the free induction decay for compensating sample heating effects [16]. The CPMG frequency (ν_{CPMG}) is determined by the number of ^{15}N CPMG π-pulses applied during the T_{relax} period, according to the relation given by [15]

$$\nu_{cpmg} = \frac{1}{2(2\tau_{CP} + t_{180,N})} \quad (1)$$

where $2\tau_{CP}$ is the spacing between successive ^{15}N CPMG π pulses.

In our experiment the pulse width was $t_{180,N}$=90 μs. We have varied ν_{CPMG} between 33.33 and 1000 Hz. Spin lock fields of the proton used were between 8.5 and 11 kHz range, and the RF amplitude is fine-tuned for each ν_{cpmg} value in order to ensure that the integral number of ^1H π pulses can be accommodated within T_{relax}. Equilibration delay of τ_{eq}=5 ms was used before and after the water alignment as was reported [15]. For, ν_{CPMG}=33.33–100 Hz and ν_{CPMG}=800–1000 Hz the data was collected in triplicate for purposes of error calculation. One experiment with no CPMG relaxation delay was also recorded as a control (i.e. T_{relax}=0). For each backbone amide ^{15}N residue, the effective transverse relaxation rate, $R_{2,eff}$, as a function of ν_{cpmg} was calculated as [25, 26]

$$R_{2,eff}(\nu_{cpmg}) = \frac{1}{T_{relax}} \ln\left[\frac{I_{CPMG}}{I_0}\right] \quad (2),$$

where T_{relax}=30 ms relaxation delay and $I(\nu_{cpmg})$ is the peak intensity for the particular CPMG frequency and peak intensity in the control spectrum recorded (T_{relax}=0) is I_0.

NMR data were processed in NMRPIPE and motional parameters were extracted. For the CPMG relaxation dispersion experiments, uncertainties in the measured $R_{2,eff}$ were calculated using

$$\Delta R_{2,eff}(\nu_{cpmg}) = \frac{1}{T_{relax}} \ln\left[\frac{\Delta I}{I(\nu_{cpmg})}\right] \quad (3),$$

where ΔI is the average standard deviation obtained from two sets of triplicate points mentioned before. For each residue CPMG relaxation dispersion trajectories at 500 and 800 MHz $^{\lambda}H$ frequency were used to calculate corresponding exchange contributions to ^{15}N R_2 according to $R_{ex} = R_{2,eff}(\nu_{cpmg}=0) - R_{2,eff}(\nu_{cpmg}=1000)$. This analysis has identified regions undergoing significant chemical exchange.

2.3. Gel filtration of recombinant PfP2

AKTA FPLC from GE Healthcare was used for gel filtration which was coupled to UV spectrometer. The gel filtration profile of recombinant PfP2 at pH 7.4 and pH 2.0 and urea denatured protein was determined using Superdex-75 column, using appropriate concentrations; 90 fractions were collected. The parameters used for gel filtration were: pressure 0.5 MPa, column bed volume 120 ml, flow rate: 0.5 ml/min. All runs were done under reduced condition (5 mM DTT) at room temperature. The profiles were then compared with profiles of marker-proteins run on the same column.

2.4. Mass spectrometry of PfP2 using MALDI-TOF

The tetramer and the monomer fraction from the gel filtration profile was collected and subjected to mass spectrometry using MALDI from Bruker Corporation (model number 201344). The protein was dissolved in phosphate buffer, pH 7.4 and glycine buffer at pH 2.0, and reconstituted using 50% acetonitile and 0.1% TFA (500 μl of 100% acetonitrile 499 μl of distilled water + 1 μl of TFA). The reconstituted protein was loaded on a MALDI plate using saturated solution of α-cyanohydroxylcinnamic acid (Bruker 201344) (20 mg/ml) in 50% acetonitrile and 0.1% TFA.

2.5. Circular dichroism (CD) spectroscopy

The spectra in the far-UV CD (190–260 nm) and the near-UV CD (260–360 nm) regions were obtained on a JASCO-810 spectropolarimeter for observing the alterations in the secondary and tertiary structure of the protein. The concentrations of protein and path lengths used were 50 μM and 0.2 cm, respectively for the far-UV CD experiments, and 50 μM and 1 cm, respectively for near-UV CD experiments. The spectropolarimeter was thoroughly purged with nitrogen gas before starting the experiments. Each spectrum was baseline corrected and was taken as an average of three accumulations at a scan rate of 50 nm min^{-1}, and a response time of 1 s. The molar ellipticity [θ] was calculated from the observed ellipticity θ as

$$[\theta] = 100 \cdot \left(\frac{\theta}{c \cdot l}\right) \quad (4)$$

where c is the concentration of the protein in M (mol dm^{-3}) and l is the path length of the cell in centimeters.

2.6. Fluorescence spectroscopy

The intrinsic fluorescence properties of the proteins were studied on a Cary Eclipse spectrofluorimeter with a 3 mL quartz cell of 1 cm path length. The concentration of PfP2-tetramer and PfP2-monomer was kept at 0.063 mM and 0.030 mM in the steady state fluorescence experiments. The excitation and emission slit widths were fixed at 5 nm. For ANS binding experiments, the ANS

concentration was kept at 0.047 mM which was determined using an extinction coefficient value of 5000 M^{-1} cm^{-1} [17]. The excitation wavelength was set at 365 nm to selectively excite the ANS molecules, and the emission spectra were monitored in the wavelength range of 400–600 nm. The emission spectra of the protein-ANS solutions were subtracted from the buffer-ANS blanks, and an average of three accumulated scans was recorded as the final graph.

2.7. Isothermal titration calorimetry

The values of thermodynamic parameters accompanying the binding of ANS with PfP2-tetramer were determined using an isothermal titration calorimeter (VP-ITC, Microcal, Northampton, MA, USA) at $T=25$ °C. The ANS solution, taken in the syringe, was titrated into the sample cell in aliquots using a 250 μl rotating stirrer-syringe, and the reference cell contained the buffer. Each experiment consisted of 50 consecutive injections of 5 μl of the ANS solution into the sample cell containing PfP2-tetramer. The duration of each injection was kept at 10 s with a 4 min interval between the consecutive injections. Origin 7.0 software, provided by Microcal was used to analyse the titration heat profiles. The total heat content Q of the solution contained in the active cell volume V_o (determined relative to zero for the unliganded species) at fractional saturation Θ after the ith injection is determined from [18],

$$Q = n\Theta M_t \Delta H \cdot V_o \quad (5)$$

where M_t is the total concentration of the protein, n is the number of binding sites in the macromolecule and ΔH is the molar heat of drug binding. The heat released $\Delta Q(i)$ from the ith injection for an injection volume dV_i is then given [18] by the following equation:

$$\Delta Q(i) = Q(i) + \frac{dV_i}{V_o}\left[\frac{Q(i)+Q(i-1)}{2}\right] - Q(i-1) \quad (6)$$

The thermodynamic parameters thus obtained associated with the binding process are binding constant (K), enthalpy of binding (ΔH), entropy of binding (ΔS), and stoichiometry of binding (n), which were determined by the best fit of the chosen model to the experimental data points.

2.8. Modelling

A model for the PfP2-tetramer was generated starting from the published dimeric structure of human P2 and the experimental constraints derived in the present study. First, the sequence of human P2 was mutated to match that of PfP2 sequence using swissPDB viewer [19]. Then the resulting dimer was energy minimized. Next, by including constraints of contacts between two dimers, derived from Rex data we docked two units of dimers by using ZDOCK [20] to arrive at a model structure for PfP2 tetramer.

3. Results and discussion

3.1. PfP2-forms a tetramer at physiological pH at micro-molar concentrations

We have recorded gel filtration profile of recombinant PfP2 at 64 and 350 μM concentrations at pH, 7.4. In both cases the profiles were similar and Fig. 1A shows the chromatograms obtained with protein concentration of 350 μM. For comparison the profile obtained for BSA marker (66 kDa) is also shown as seen in Fig. 1B. From this it can be seen that PfP2 forms a stable tetramer in solution. This fraction pool of PfP2 was subjected to MALDI for

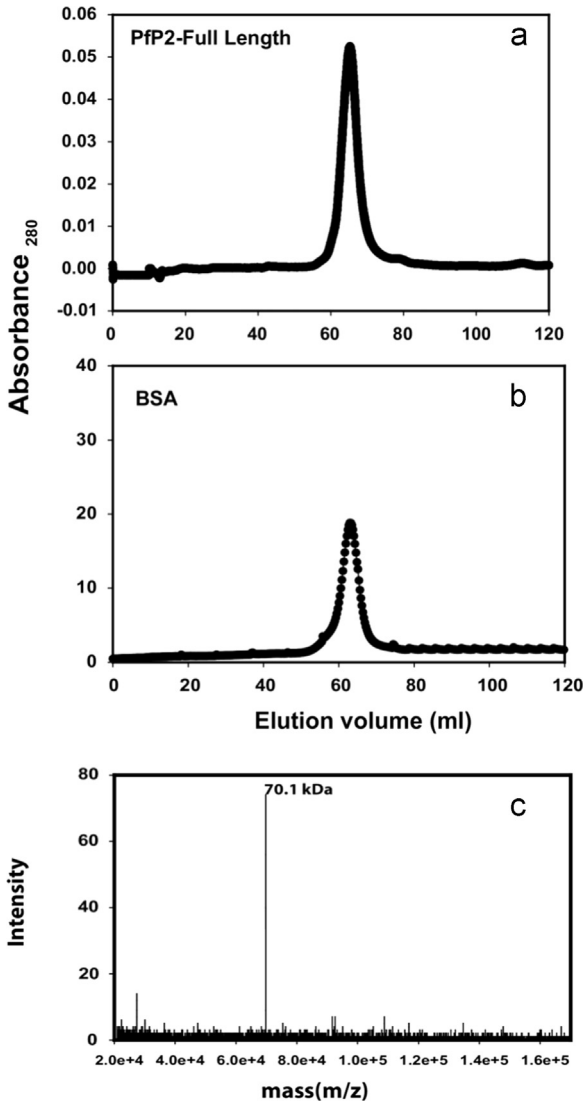

Fig. 1. Gel filtration profiles: (A) recombinant PfP2 (loading:1 ml of 4 mg/ml); (B) BSA protein marker (loading:1 ml of 1 mg/ml) run on the same column; (C) MALDI spectrum of deuterated $^{2}H/^{13}C/^{15}N$ PfP2 tetramer.

an accurate estimate of molecular size, and a mass of 70.1 kDa was observed (Fig. 1C). This was for triply labelled ($^{2}H/^{15}N/^{13}C$) PfP2-tetramer.

3.2. PfP2 forms a molten globule monomer at pH 2

Fig. 2 shows the FPLC chromatogram of PfP2 at pH 2. It can be clearly seen that the molecule is a monomer with a molecular weight of 15.5 kDa.

The CD spectra of the protein under the same conditions, shown in Fig. 3A, indicate that the protein has prominent helical structure as indicated by bands at 208 and 222 nm and very less tertiary structure as indicated by low ellipticity in the region 260–340 nm. Further, we observe that ANS, a dye which is known to bind strongly to partially folded states or molten globule states of proteins [17,21,22], binds to PfP2 at pH 2 as shown in Fig. 3B; the dye exhibits very little fluorescence in free solution or when the protein is fully denatured in 8 M urea, but shows very high fluorescence when added to solution containing PfP2 monomer alone at pH 2. Moreover, the $^{1}H–^{15}N$ HSQC spectrum of the protein in Fig. 3C shows only ~40 peaks as against the expected 138 peaks for the full protein. This can be attributed to ms-μs time scale

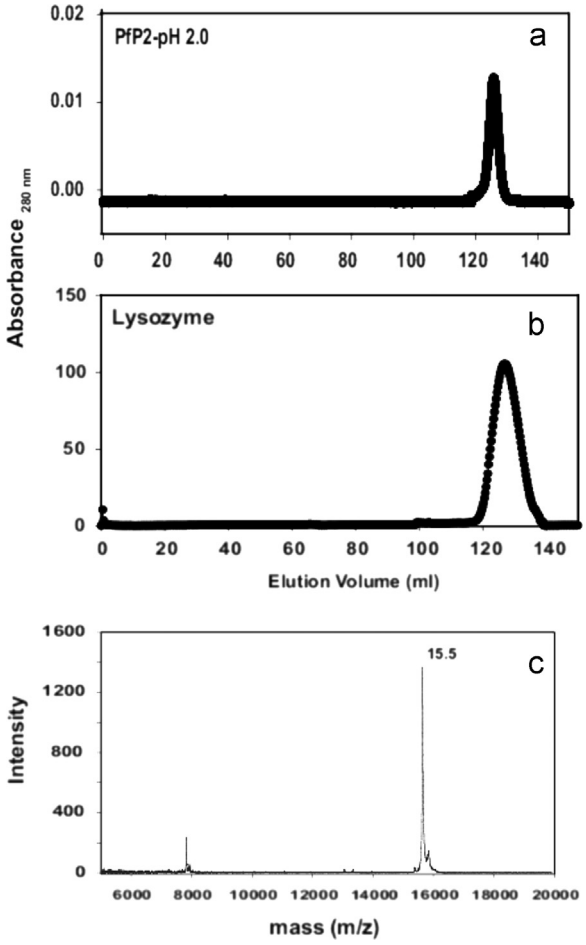

Fig. 2. Gel filtration profiles: (A) recombinant PfP2 at pH 2.0 (loading: 1 ml of 2 mg/ml); (B) Lysozyme protein marker (loading:1 ml of 1 mg/ml) run on the same column; and (C) MALDI spectrum of unlabelled PfP2 monomer.

dynamics in major portion of the protein which results in disappearance of the peaks belonging to those residues. All these observations are indicative of a molten globule like structure for the PfP2 monomer at pH 2.

3.3. Structural features of PfP2-tetramer

3.3.1. Secondary and tertiary structural characteristics

Recently, we have described structural characterization of PfP2 at a rather high concentration (mM) where it was seen to form a mixture of oligomers, the predominant species being an octamer [7]. This involved CD and NMR studies. Interestingly, the present observations on the pure tetramer coincide almost entirely with those and thus the conclusions regarding some general characteristics can be extrapolated here as well. For purpose of ready comparison, we show here the circular dichroism (CD) (Fig. 4A) and HSQC (Fig. 4C) spectra of the tetramer. One can see that the far-UV CD spectra (Fig. 4A) at pH 7.4 showed two negative bands at 210 nm and 222 nm which are indicative of helical structures. The near-UV CD spectra of PfP2 (Fig. 4B) at pH 7.4 showed weak ellipticity in the wavelength range of 260–280 nm, indicating that the tetramer has a loose tertiary structure.

Likewise, the HSQC spectrum shown here overlays exactly with that reported previously [7] and thus the assignments of the individual peaks can be readily transferred. The HSQC spectrum shows only 43 peaks and these belong to the C-terminal residues of the polypeptide chain. Secondary shift calculations reported earlier [7,8] can also be transferred to the present case and we conclude that the C-terminal segment is devoid of any secondary structural preferences.

3.3.2. Hydrophobic surfaces in PfP2-tetramer

The presence of hydrophobic surfaces/pockets in proteins is often probed by binding of ANS, which being hydrophobic in nature can selectively access such regions in the protein, and optical properties are very sensitive to the polarity of its microenvironment. Enhanced emission intensity upon binding with nonpolar surfaces has been observed [22,23], when excited at 365 nm. In the presence of a partially folded protein with exposed hydrophobic surfaces, the fluorescence emission intensity is enhanced and the emission maximum is blue shifted compared to that of free ANS [21]. Fig. 5A shows the fluorescence emission spectra of 0.047 mM ANS, in the presence of native PfP2-tetramer (concentration: 0.063 mM) and upon urea denaturation at pH 7.4. We observed that ANS binding to the protein is maximum in its native state (absence of urea) and decreases gradually when the urea concentration is increased from 1 M to 8 M.

Isothermal titration calorimetry (ITC) provides valuable information on binding of ligands to proteins. A representative isothermal titration calorimetric profile for the binding of 15 mM ANS with 0.075 mM protein at pH 7.4 and 25 °C is shown in Fig. 5B; this is a resultant of 50 injections to ensure full saturation of the binding sites. Each peak in the binding isotherm represents a single injection of ANS into the protein solution. The lower panel of Fig. 5B shows the plot of heat change per injection as a function of the molar ratio of ANS to PfP2-tetramer.

From the above data, it appears that ANS is able to find more than one binding sites on PfP2-tetramer with varying degrees of exothermicity. A sequential two-binding sites model fitted the data with the values of binding constants of $(9.84 \pm 0.2) \times 10^3$ and $(172 \pm 2.7)\ M^{-1}$ and binding enthalpies of (8.5 ± 0.2) kJ mol^{-1} and $-(0.28 \pm 0.04)$ kJ mol^{-1}, respectively. The major binding event (K1) is accompanied by an endothermic enthalpy of binding with a gain in entropy; out of the two binding events only one corresponding to K2 shows exothermic binding effects. ANS is known to bind the partially folded states of proteins both via hydrophobic and ionic interaction due to its molecular properties. The ionic interactions contribute to the exothermic heating effects whereas hydrophobic interactions impart endothermic contribution.

The thermodynamic parameters obtained from the ITC measurements permit insights into the factors that contribute to the complexation of ANS to the loosely compacted state of PfP2-tetramer. The major binding event which is accompanied by endothermic enthalpy and positive entropy is suggestive of hydrophobic interactions. The minor event which is exothermic in nature can be attributed to weak ionic interactions.

To gain residue specific information with regard to the hydrophobic pocket, we recorded 2D ^{1}H–^{15}N HSQC spectra on native deuterated PfP2-tetramer with and without ANS (Fig. 5C). We do not observe chemical shift changes for most of the residues in the C terminal on addition of ANS, indicating that the C-terminal domain does not interact with ANS. In other words, the hydrophobic pocket is constructed by the N-terminal portion of the protein.

3.3.3. Molten globule structure is preserved in the tetramer

The circular dichroism spectrum of the tetramer in the far UV region showed a very weak band at 280 nm and overall the signal is very weak. This gave an indication that the tertiary structure in the tetramer is perhaps not very rigid. Similar conclusion is also evident from the NMR data as follows. The molecular weight of the tetramer is 62 kDa. This is not such a large molecular mass that the NMR signals become non observable due to slow tumbling

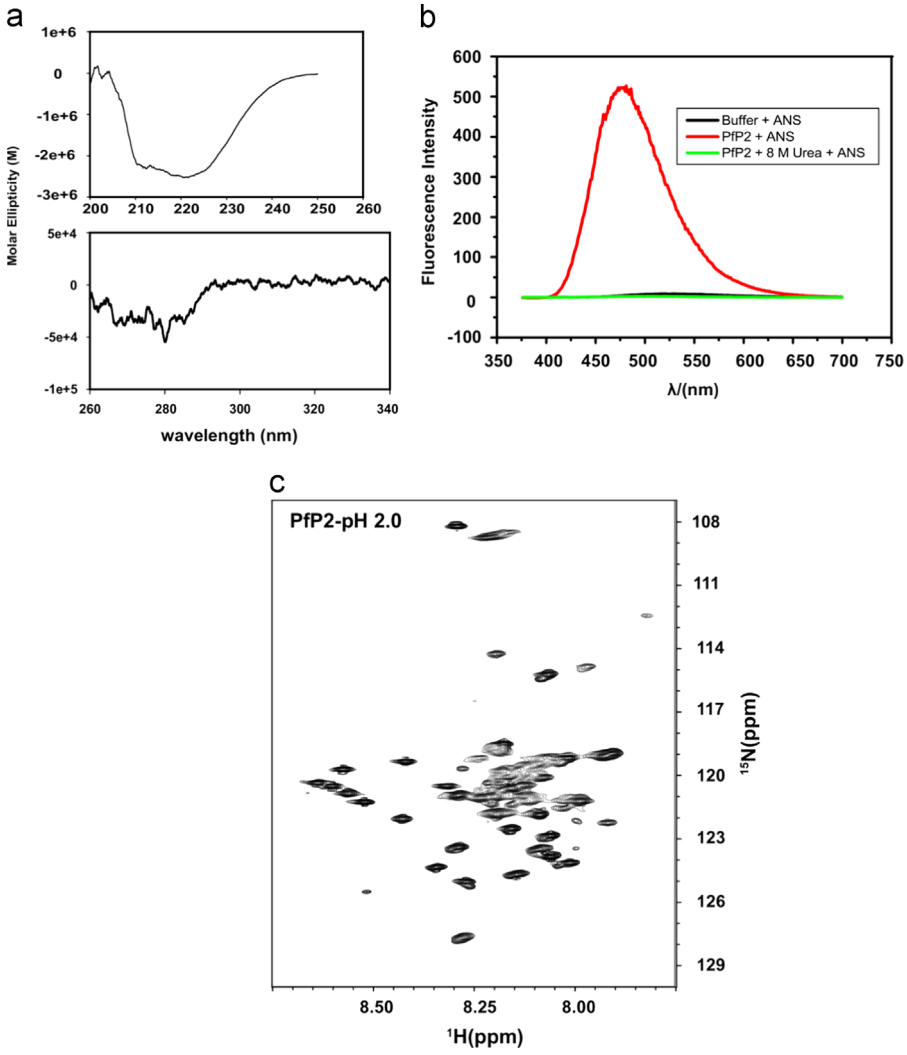

Fig. 3. PfP2-monomer spectra at pH 2.0: (A) far-UV CD spectrum of 50×10^{-3} mM PfP2 (top panel), and near-UV CD spectrum of 50×10^{-3} mM PfP2 (bottom panel); (B) Fluorescence emission spectra of 0.047 mM ANS, with 0.030 mM PfP2-monomer (red), with buffer alone (black), and with denatured PfP2 in 8 M urea (green); (C) 2D ^{1}H–^{15}N HSQC spectrum of PfP2-monomer at 25° C at pH 2.0.

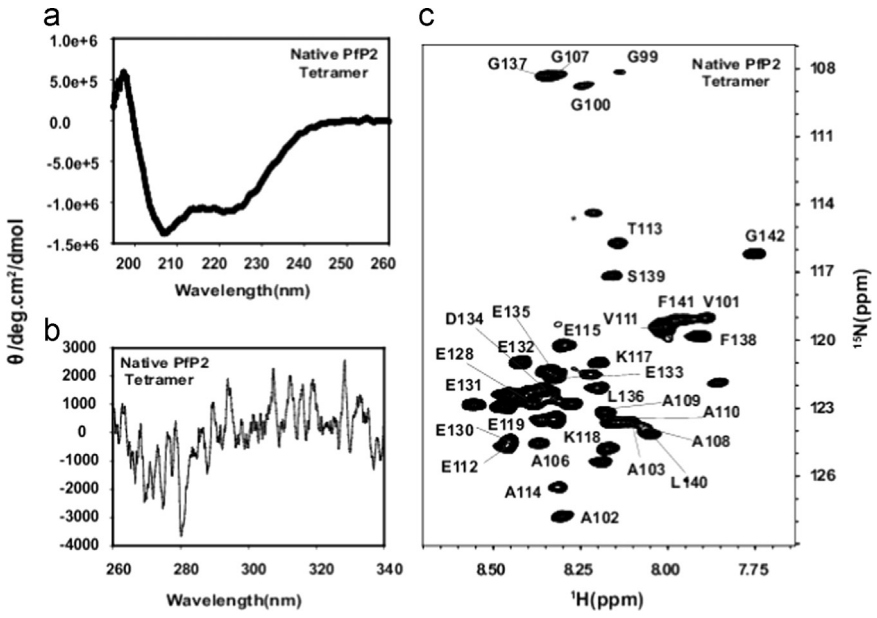

Fig. 4. PfP2 tetramer spectra at pH 7.4: (A) far-UV CD spectrum of 50×10^{-3} mM PfP2 and (B) near-UV CD spectrum of 50×10^{-3} mM PfP2; (C) 2D ^{1}H–^{15}N HSQC spectrum of PfP2-tetramer at 25° C at pH 7.4.

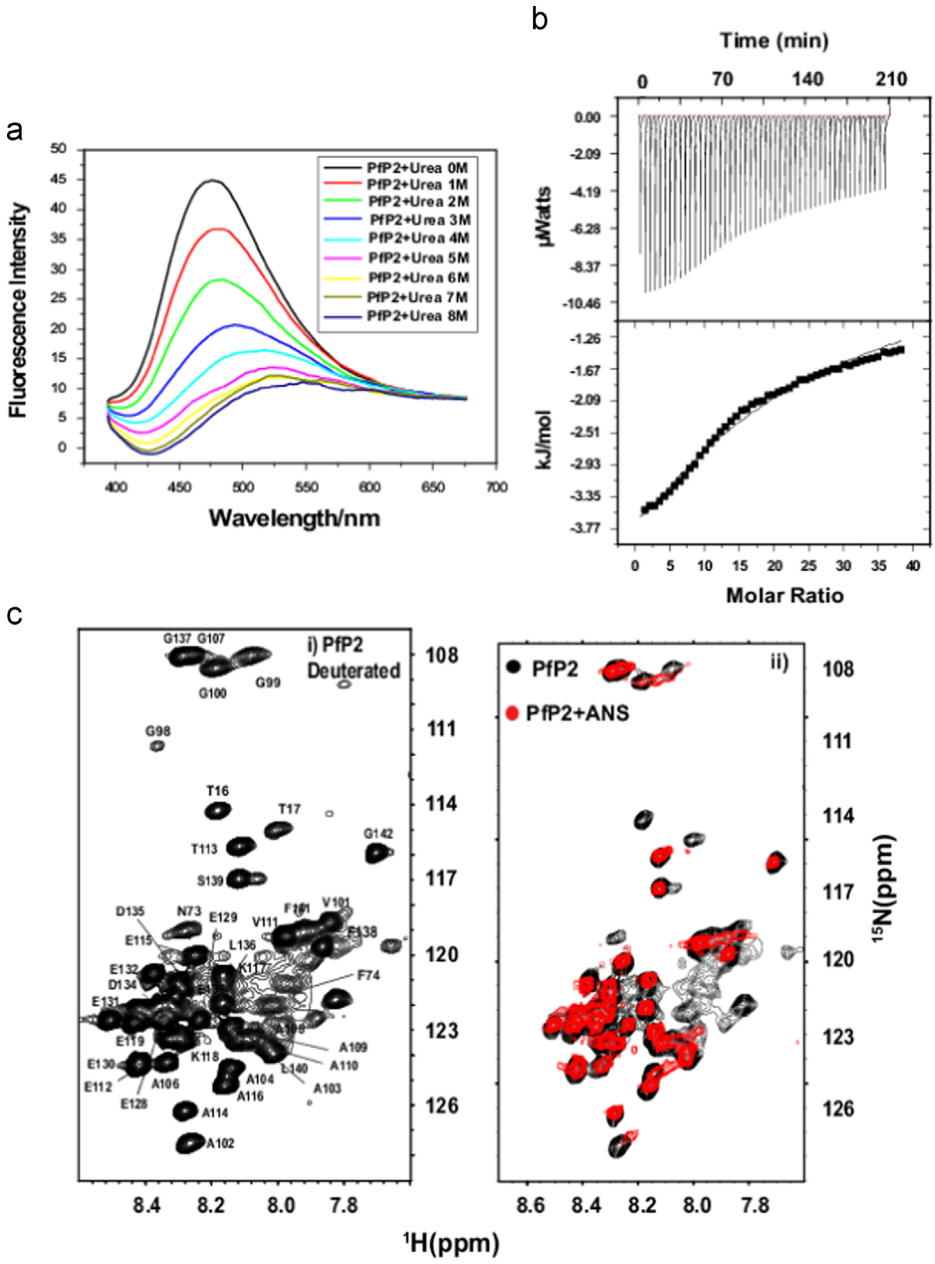

Fig. 5. ANS binding to PfP2 tetramer. (A) Fluorescence emission spectra of 0.047 mM ANS, with 0.063 mM PfP2-tetramer in the presence of varying urea concentrations from 0 M to 8 M at pH 7.4. (B) Raw data for the titration of 15 mM ANS in 0.075 mM PfP2 at pH 7.4 and 25 °C showing the calorimetric response as successive injections of ligand are added to the sample cell (upper panel). The lower panel shows the integrated heat profile of calorimetric titration. (C) 2D ^{1}H–^{15}N HSQC spectrum at 25° C of: (i) deuterated PfP2-tetramer at pH 7.4, (ii) Overlay of spectra of PfP2 with and without ANS. Protein: ANS ratio was 1:30. The spectra were recorded on a Bruker 800 MHz NMR spectrometer.

motions. In fact, the C-terminal segments from each of the chains in the tetramer do produce signals, and that of course indicates high flexibility of this domain. Deuteration of the chain did not produce any more peaks in the spectrum. This indicates that vanishing of the signals, for the core of the tetramer is due to other reasons and most naturally, that must be slow fluctuations in the packing of the helices in the core.

A further insight comes from comparison of the HSQC spectrum of the tetramer with that of the monomer observed at pH 2. It is interesting to note that in both cases the number of peaks observed in the spectra are nearly the same. Some peaks appear to be shifted, but this must be attributed to protonation of some side chains (eg, Glu and Asp) at low pH. Thus, combining both CD and NMR observations, we can safely conclude that the molten globule nature of the monomer is preserved in the tetramer.

3.4. Elucidation of step-wise assembly of tetramer

To gain insights into the assembly of the tetramer we adopted the strategy of systematic dissociation of the tetramer using urea as the dissociating agent and monitor the changes that occur in the spectra. Previous studies on the octamer had indicated that the denaturation transition by urea occurs in the concentration range, 3–7 M urea at pH 5.6 [8]. Therefore, we decided to focus attention to the range 4–6 M urea and monitored the step-wise dissociation using FPLC, and this was done at two pH values, 5.6 and 7.4. It turned out that the results are identical in the two cases and here we show the results at pH 5.6. Fig. 6 shows the FPLC chromatograms at the three concentrations.

The FPLC profiles indicate that at 4 M urea there is a pure tetramer, at 5 M urea a small population of dimer appears, and at

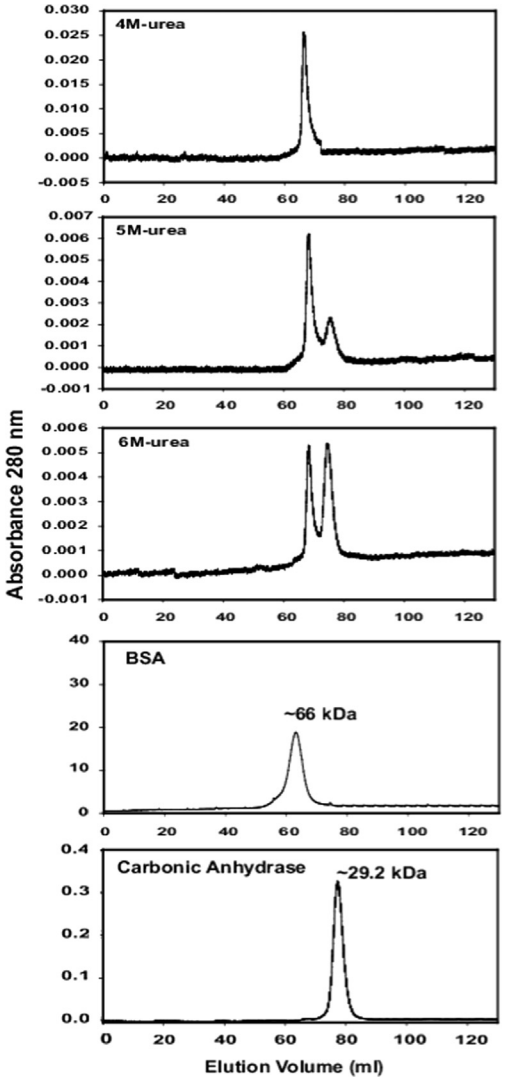

Fig. 6. Urea dependent Gel filtration profiles of PfP2: Gel filtration profiles of recombinant PfP2 at 4 M, 5 M and 6 M urea at pH 5.6 with markers BSA and carbonic anhydrase run on the same column with loading concentrations of 200 μM.

6 M the two populations become nearly equal. These are in exchange, as could be evidenced by the fact that collection of one of the fractions, concentrating it and rerunning the FPLC resulted in the same pattern. This indicates that in this range, the tetramer dissociates via a dimer. At higher urea concentrations such as at 9 M, the dimer further dissociates into monomers. Thus the assembly process would occur as, monomer–dimer–tetramer.

In the 2D ^{1}H–^{15}N HSQC spectra as shown in Fig. 7 under these conditions there is a gradual change in the number of peaks, the number decreasing from 6 M urea, where we observe all the expected peaks, to 4 M urea, at which stage we observe only the peaks from the C-terminal. At 5 M urea, the peaks from the segment, M31-L44 are missing which belong to the first predicted helical segment [10] in the protein. This indicates that, in going from 6 M to 5 M urea an intermediate level exchange is introduced between dimer and tetramer and this must arise due to local structure formation in this segment.

3.5. ms-μs time scale dynamics identifies dimer association sites in the tetramer

Valuable insights into structural transitions during folding/unfolding of a protein can be derived from studying ms-μs time scale motions which can be obtained from relaxation dispersion measurements [15]. We carried out such measurements as described in Section 2 in the transition zone (4–6 M urea) of unfolding profile of PfP2 and these are described below. In these experiments, $R_{2,\mathrm{eff}}$ is plotted against the ν_{CPMG} and in the presence of exchange, $R_{2,\mathrm{eff}}$ decays with ν_{CPMG} and it its absence there will be no dependence of $R_{2,\mathrm{eff}}$ on ν_{CPMG}. This provides an unambiguous method to identify residues undergoing conformational exchange. Since conformational exchange contribution to R_2 depends, among other things, on the chemical shift frequency separation between the exchanging sites (i.e. between the two conformations), exchange seen for a particular residue at one field may not be seen at another, so in order to be more exhaustive we have recorded these experiments at two fields. Residue specific relaxation dispersion trajectories on backbone ^{15}N spins were recorded at 500 MHz and 800 MHz (^{1}H frequency) for PfP2 at 5 M and 4 M urea concentrations. Fig. 8A–C shows plots of $R_{2,\mathrm{eff}}$ at 4 M and 5 M urea condition.

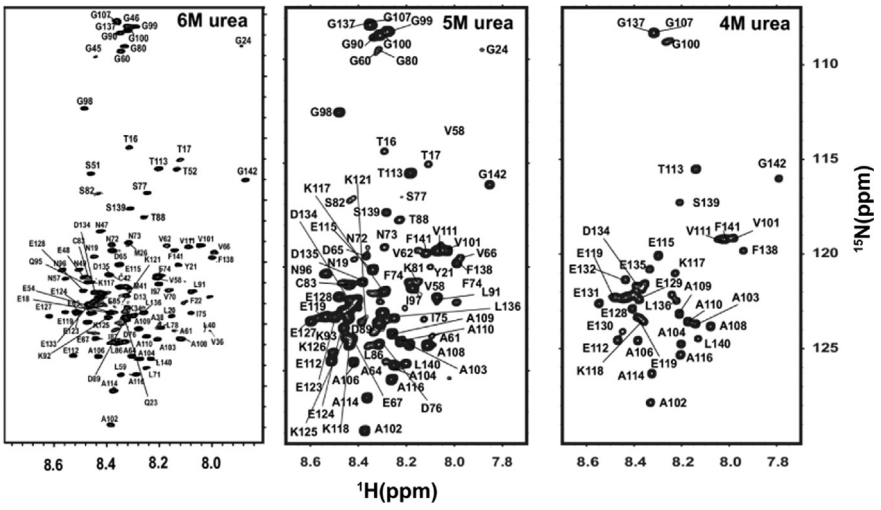

Fig. 7. Urea dependent ^{1}H–^{15}N HSQC spectra of PfP2: Urea concentrations are indicated in the individual panels and the assignments have been marked; pH=5.6 and temperature=25° C.

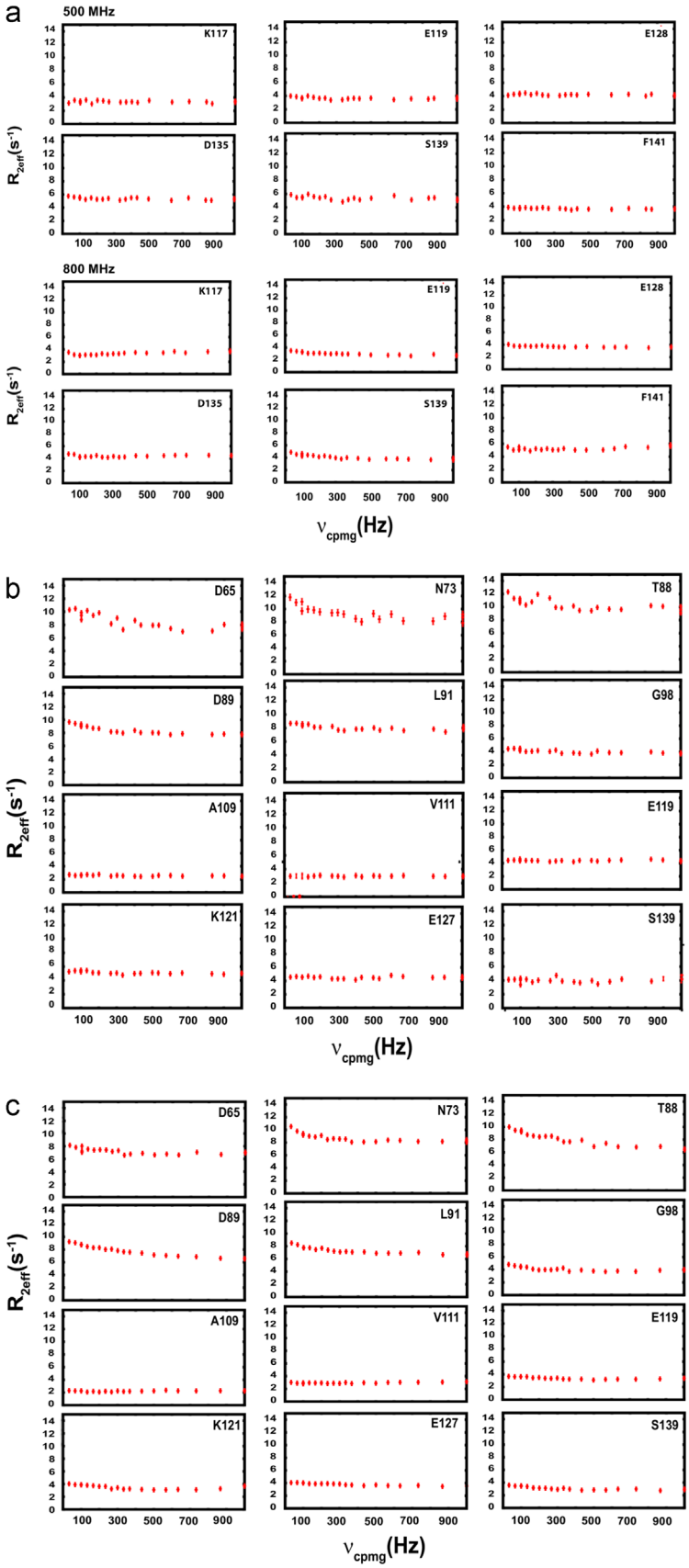

Fig. 8. 15N –CPMG relaxation dispersion trajectories for representative residues of PfP2:(A)in 4 M urea recorded at 500 MHz and 800 MHz spectrometer frequencies; (B) in 5 M urea recorded at 500 MHz; (C) in 5 M urea recorded at 800 MHz at pH=5.6 in all cases.

From these data, R_{ex}, the conformational exchange contributions at the two conditions were calculated as described in Section 2 and these results are shown in Fig. 9. It is observed that at 4 M urea where only the C terminal signals are seen, R_{ex} is almost non-existent. Interestingly, this is also true for this segment under 5 M urea condition. However, at 5 M urea, there is a substantial contribution in the central segment (50–90) and this varies along the sequence. In Fig. 9 we also show as insets CD spectra at 5 M and 4 M urea and the observed ellipticities yielded helical contents of 35% and 40%, respectively, the latter being the helical content even in the absence of urea; note that this also matches with the predicted helical structure indicated on the top of the figure. Remembering the FPLC results that at 5 M urea there is equilibrium between dimer and tetramer, we infer that dimer–tetramer exchange must be contributing to the high R_{ex} seen here and these regions therefore identify the sites of association of the two dimers forming the tetramer. We reiterate here that at 5 M urea the peaks belonging to another segment of the protein, namely, M31-L44, disappear and this must be attributed to intermediate exchange time scale folding transitions in that segment inside the dimers and the tetramers. Similarly, when we go from 5 M to 4 M area the residues in the central segment which had high R_{ex} values disappear and this must be attributed again to intermediate exchange time scale folding transitions in those regions. This is typical hydrophobic collapse model of protein folding, wherein the secondary structure forms follows collapse of the chain into a compact form.

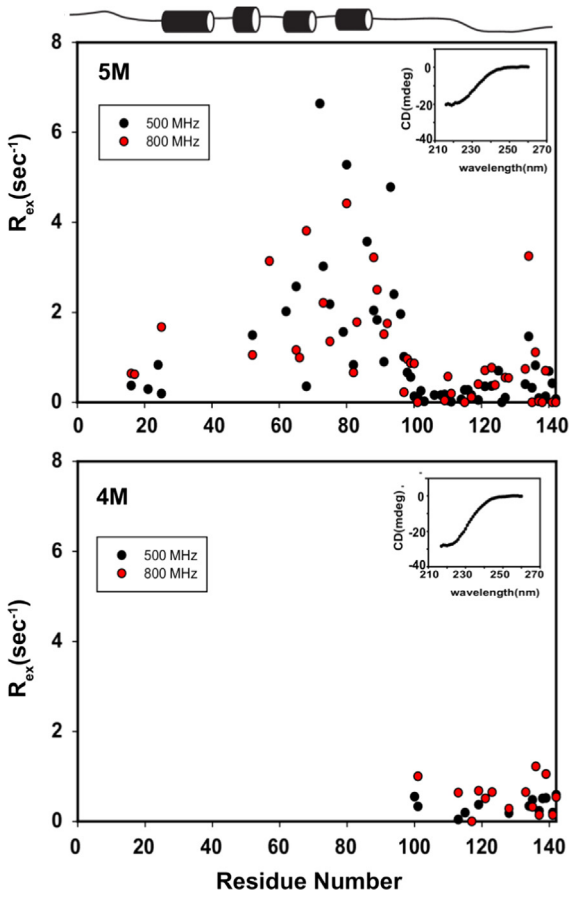

Fig. 9. Plot of R_{ex} vs residue number: The measured values at pH 5.6 and at two different urea conditions, 5 M and 4 M are shown at 500 and 800 MHz spectrometer frequencies. The R_{ex} values for individual residues were determined as described in the materials and methods. Cylinders on the top show predicted PfP2 helical structures (~40%) while inset shows observed CD ellipticity which indicates increase in helicity from 35% at 5 M urea to 40% on diluting to 4 M urea.

3.6. Structural similarities and dissimilarities between PfP2 and HuP2

Recently, the structure of human P2 (HuP2) devoid of the C-terminal 50 residues determined by NMR spectroscopy at pH 7.5 has been published [4]. The structure of heterodimer of human P1 and P2 full length proteins has also been published [24], and interestingly, the folded dimer structures are nearly identical in both. The C-terminal segment is seen to be flexible and the dimers are formed by packing of four helices (α1–α4) from each of the monomers. The α1 helices from the two monomers form the core of the dimer while the other helices (α2, α3, α4) lie on the outer surface. The packing of the helices is such as to maximize interactions and we observe that α1 and α4 helices from the two monomers run in opposite directions. PfP2, unlike human P2, forms a tetrameric structure at pH 7.4 and is a monomer at pH 2 and in both situations the monomeric units are molten globules; The ^{1}H-^{15}N HSQC spectrum of PfP2 tetramer shows only 43 peaks as against all the peaks seen in the case of human P2. The tetramer is formed by self-association of two dimers as described above. On the other hand the sequence similarity between HuP2 and PfP2 in the region (residues 1–75) is 70% and which forms a well folded stable dimer. Further, the secondary structural elements observed in HuP2 and the predicted ones in PfP2 are identical; the total helical content derived from the predicted secondary structure in PfP2 matches the helical content derived from CD data quite closely. In PfP2, the predicted helical segments are α1, 33–44; α2, 50–60; α3, 67–78; α4, 82–92. This numbering corresponds to the recombinant protein used here, which has additional 30 residues at the N-terminal. Therefore these respective numbers in native PfP2 would be as listed below and these must be compared with those in human P2.

PfP2: α1, 3–14; α2, 20–30; α3, 37–48; α4, 52–62

HuP2: α1, 4–14; α2, 20–31; α3, 36–47; α4, 51–59

In HuP2 dimer α1, α1′ are in the core of the dimer. This is indeed the prediction in PfP2 on the basis of R_2 data and AABUF calculations[7, 8] as described previously. Thus we can infer that the structure of the dimer in the tetramer of PfP2 is very similar to the dimer structure of HuP2. On this premise we have built a model for PfP2 tetramer starting from the HuP2 dimer structure using the contact regions between the two dimers as described above. This is described below.

3.7. Structural model for PfP2 tetramer

Considering that assembly of the PfP2 tetramer proceeds as monomer-dimer-tetramer, and noting that the dimer structure of HuP2 is essentially preserved in the PfP2 tetramer, we begin with the HuP2 dimer structure. We then generated the dimer of PfP2 by mutating the residues in HuP2 dimer structure to match the PfP2 sequence using swissPDB viewer [19]. Then the resulting dimer was energy minimized. This structure is shown in Fig. 10A. We observe that as a result of mutation some of the residues which were involved in helix formation in α4 in HuP2 have opened up in PfP2 dimer. Fig. 10B shows an overlay of HuP2 and PfP2 dimers.

Next, by including constraints of contacts between two PfP2 dimers, derived from R_{ex} data as mentioned in the previous sections, we docked two units of dimers by using ZDOCK [20]. This is a rigid body modelling algorithm, uses shape complementarity, desolvation and electrostatic energy contributions between two protein molecules and searches through the three dimensional space to find the most energetically favourable arrangement using a Fast Fourier Transform (FFT) based scoring procedure. The resulting structure for the PfP2 tetramer is shown in Fig. 10C. Two different views are shown to display the interaction sites clearly. As can be seen the dimeric structures are not perturbed by the

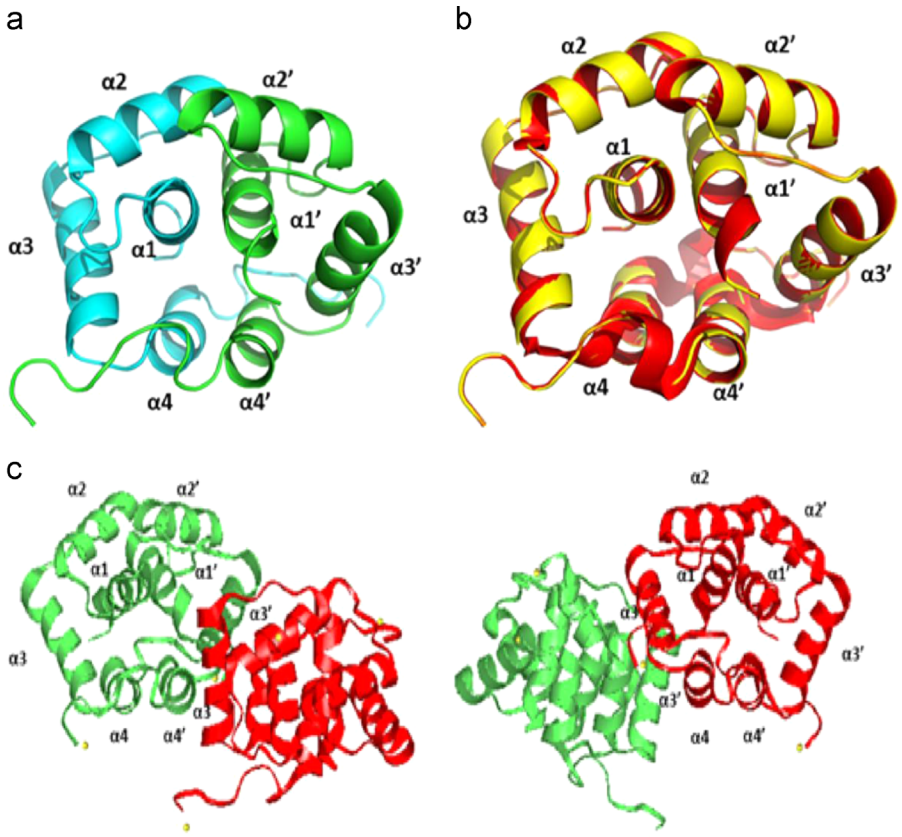

Fig. 10. Structure of PfP2:(A) PfP2 dimer obtained from HuP2 structure by mutating the HuP2 sequence with that of PfP2. (B) Overlay of structure of HuP2 homodimer (red) on PfP2 dimer structure (yellow); (C) Structure of PfP2 tetramer derived using ZDOCK protein docking software. Green and red represents two homodimers of PfP2. Two views are shown. On the left, helices in green dimer are marked and on the right, helices in the red dimer are marked.

association process, and the interface is formed by (α3, α4) and (α3′,α4′) helices of the two dimers. The α4′ helix of one dimer (green) comes close in contact with the α3 helix (red) of another dimer (see left panel). Similarly, α3′ of one dimer (green) is in close contact with α4 of another dimer (red) (see right panel). The helices are closely packed at the interface.

4. Concluding remarks

We have demonstrated that *Plasmodium falciparum* P2 exists as a stable tetramer as a basic unit in solution at micromolar concentration and at pH 7.4. The individual monomers in the tetramer have molten globule like characteristics. The tetramer contains hydrophobic pockets contributed by the N terminal segments of the protein, the C terminal 40 residues remain unstructured and flexible. From the NMR structure determination point view there was a great challenge since the native tetramer displays only ~40 peaks which belong to the flexible C-terminal domain of the protein. Using a strategy of partially unfolding the tetramer for observing NMR signals from all the residues and gathering insights into structural and motional transitions, we have been able to demonstrate that the assembly of the tetramer occurs as, monomer–dimer–tetramer. Relaxation dispersion measurements at 5 M urea concentration have shown that the central region (50–90) exhibits high conformational exchange on ms-μs time scale and these indicated the contact points for association of two dimers to form the tetramer. From these data we have been able to build a model for the structure of the tetramer using the published dimeric structure of HuP2 as the starting point.

It is very interesting to note that PfP2 and HuP2 which have 69% sequence homology in the full length proteins have a basic difference with regard to the overall behaviours: HuP2 forms a stable dimer at pH 7.5 while PfP2 forms a molten globule like tetramer under the same conditions. This may have functional implications. HuP2 is solely a ribosomal protein where it remains in an associated state as a dimer in the ribosomal stalk. On the other hand, PfP2 has both ribosomal and non-ribosomal functions and the latter seem to involve various types of associated states of the protein. In the parasite, multiple oligomers are seen during the nuclear division and the homo-tetramer is translocated to the red blood cell surface in infected cells. Thus we speculate that the molten globule like nature of PfP2 structure facilitates structural rearrangements as required by different kinds of functions.

Author contributions

PM, SC, SM and DS carried out the experiments, PM, SS and RVH designed all the studies and contributed in writing the manuscript. All authors have given approval to the final version of the manuscript.

Acknowledgements

We thank TIFR, DAE, for funding and the National Facility of High Field NMR at TIFR for making possible the NMR studies. All authors have declared no conflict of interest.

Appendix A. Transparency document

Transparency document associated with this article can be found in the online version at http://dx.doi.org/10.1016/j.bbrep.2015.03.010.

References

[1] M. Tchorzewski, B. Boldyreff, O.G. Issinger, N. Grankowski, Analysis of the protein-protein interactions between the human acidic ribosomal P-proteins: evaluation by the two hybrid system, Int. J. Biochem. Cell Biol. 2 (2000) 737–746.

[2] T. Uchiumi, R. Kominami, Binding of mammalian ribosomal protein complex P0 center dot P1 center dot P2 and protein L12 to the GTPase-associated domain of 28S ribosomal RNA and effect on the accessibility to anti-28S RNA autoantibody, J. Biol. Chem. 272 (1997) 3302–3308.

[3] S. Das, H. Basu, R. Korde, R. Tewari, S. Sharma, arrest of nuclear division in *Plasmodium* through blockage of erythrocyte surface exposed ribosomal protein P2, PLoS Pathog. 8 (2012) e1002858.

[4] K.M. Lee, C.W.H. Yu, D.S.B. Chan, T.Y.H. Chiu, G.A. Zhu, K.H. Sze, P.C. Shaw, K. B. Wong, Solution structure of the dimerization domain of ribosomal protein P2 provides insights for the structural organization of eukaryotic stalk, Nucleic Acids Res. 8 (2010) 5206–5216.

[5] K.-M. Lee, C.W.-H. Yu, T.Y.-H. Chiu, K.-H. Sze, P.-C. Shaw, K.-B. Wong, Solution structure of the dimerization domain of the eukaryotic stalk P1/P2 complex reveals the structural organization of eukaryotic stalk complex, Nucleic Acids Res. 40 (2012) 3172–3182.

[6] L. Wawiórka, D. Krokowski, Y. Gordiyenko, D. Krowarsch, C.V. Robinson, I. Adam, N. Grankowski, M. Tchórzewski, In vivo formation of *Plasmodium falciparum* ribosomal stalk—a unique mode of assembly without stable heterodimeric intermediates, Biochim. Biophys. Acta (BBA)—Gen. Sub. (2014).

[7] P. Mishra, S. Das, L. Panicker, M.V. Hosur, S. Sharma, R.V. Hosur, NMR insights into folding and self-association of *Plasmodium falciparum* P2, Plos One 7 (2012) e36279.

[8] P. Mishra, S. Sharma, R.V. Hosur, Residue level description of in vivo self-association of *Plasmodium falciparum* P2, J. Biomol. Struct. Dyn. (2013) 1–11.

[9] A.G. Palmer III, J. Cavanagh, P.E. Wright, M. Rance, Sensitivity improvement in proton-detected two-dimensional heteronuclear correlation NMR spectroscopy, J. Magn. Reson. 93 (1991) 151–170.

[10] L. Kay, P. Keifer, T. Saarinen, Pure absorption gradient enhanced heteronuclear single quantum correlation spectroscopy with improved sensitivity, J. Am. Chem. Soc. 114 (1992) 10663–10665.

[11] J. Cavanagh, W.J. Fairbrother, A.G. Palmer III, N.J. Skelton, Protein NMR Spectroscopy: Principles and Practice, Academic Press, UK, 1995.

[12] A.G. Palmer III, NMR characterization of the dynamics of biomacromolecules, Chem. Rev. 104 (2004) 3623–3640.

[13] K. Henzler-Wildman, D. Kern, Dynamic personalities of proteins, Nature 450 (2007) 964–972.

[14] A.J. Baldwin, L.E. Kay, NMR spectroscopy brings invisible protein states into focus, Nat. Chem. Biol. 5 (2009) 808–814.

[15] D.F. Hansen, P. Vallurupalli, L.E. Kay, An improved ^{15}N relaxation dispersion experiment for the measurement of millisecond time-scale dynamics in proteins, J. Phys. Chem. B112 (2008) 5898–5904.

[16] A.C. Wang, A. Bax, Minimizing the effects of radio-frequency heating in multidimensional NMR experiments, J. Biomol. NMR 3 (1993) 715–720.

[17] L. Stryer, The interaction of a naphthalene dye with apomyoglobin and apohemoglobin: a fluorescent probe of non-polar binding sites, J. Mol. Biol. 13 (1965) 482–495.

[18] T. Banerjee, S.K. Singh, N. Kishore, Binding of naproxen and amitriptyline to bovine serum albumin: biophysical aspects, J. Phys. Chem. B110 (2006) 24147–24156.

[19] N. Guex, M. Peitsch, Swiss-PdbViewer: a fast and easy-to-use PDB viewer for Macintosh and PC, Protein Data Bank quarterly newsletter 77, 7 (1996).

[20] R. Chen, L. Li, Z. Weng, ZDOCK: an initial-stage protein-docking algorithm, Proteins: Struct. Funct. Bioinform. 52 (2003) 80–87.

[21] A.B. Rawitch, R.-Y. Hwan, Anilinonaphthalene sulfonate as a probe for the native structure of bovine alpha lactalbumin: absence of binding to the native, monomeric protein, Biochem. Biophys. Res. Commun. 91 (1979) 1383–1389.

[22] G. Semisotnov, N. Rodionova, O. Razgulyaev, V. Uversky, A. Gripas, R. Gilmanshin, Study of the molten globule intermediate state in protein folding by a hydrophobic fluorescent probe, Biopolymers 31 (1991) 119–128.

[23] R.J. Fitzgerald, H.E. Swaisgood, Binding of ions and hydrophobie probes to α-lactalbumin and casein as determined by analytical affinity chromatography, Arch. Biochem. Biophys. 268 (1989) 239–248.

[24] K.-M. Lee, K. Yusa, L.-O. Chu, C.W.-H. Yu, M. Oono, T. Miyoshi, K. Ito, P.-C. Shaw, K.-B. Wong, T. Uchiumi, Solution structure of human P1●P2 heterodimer provides insights into the role of eukaryotic stalk in recruiting the ribosome-inactivating protein trichosanthin to the ribosome, Nucleic Acids Res. 41 (2013) 8776–8787.

[25] M. Tollinger, N.R. Skrynnikov, F.A. Mulder, J.D. Forman-Kay, L.E. Kay, Slow dynamics in folded and unfolded states of an SH3 domain, J. Am. Chem. Soc. 123 (2001) 11341–11352.

[26] D.M. Korzhnev, X. Salvatella, M. Vendruscolo, A.A. Di Nardo, A.R. Davidson, C. M. Dobson, L.E. Kay, Low-populated folding intermediates of Fyn SH3 characterized by relaxation dispersion NMR, Nature 430 (2004) 586–590.